Science
AAAS

Interfollicular Epidermal Stem Cells Self-Renew via Autocrine Wnt Signaling

Xinhong Lim *et al.*

Science **342**, 1226 (2013);
DOI: 10.1126/science.1239730

References and Notes

1. Y. R. Shen, *The Principles of Nonlinear Optics* (Wiley-Interscience, New York, 1984).
2. R. Boyd, *Nonlinear Optics* (Academic Press, New York, ed. 3, 2008).
3. J. A. Armstrong, N. Bloembergen, J. Ducuing, P. S. Pershan, *Phys. Rev.* **127**, 1918–1939 (1962).
4. D. S. Hum, M. M. Fejer, *C. R. Phys.* **8**, 180–198 (2007).
5. A. Arie, N. Voloch, *Laser Photonic Rev.* **4**, 355–373 (2010).
6. A. Rose, D. R. Smith, *Opt. Mater. Express* **1**, 1232–1243 (2011).
7. X. Gu, R. Y. Korotkov, Y. J. Ding, J. U. Kang, J. B. Khurgin, *J. Opt. Soc. Am. B* **15**, 1561–1566 (1998).
8. C. Canalias, V. Pasiskevicius, *Nat. Photonics* **1**, 459–462 (2007).
9. J. Valentine *et al.*, *Nature* **455**, 376–379 (2008).
10. C. Argyropoulos, P. Y. Chen, G. D'Aguanno, N. Engheta, A. Alù, *Phys. Rev. B* **85**, 045129 (2012).
11. E. J. R. Vesseur, T. Coenen, H. Caglayan, N. Engheta, A. Polman, *Phys. Rev. Lett.* **110**, 013902 (2013).
12. S. Roke, M. Bonn, A. V. Petukhov, *Phys. Rev. B* **70**, 115106 (2004).
13. V. G. Veselago, *Sov. Phys. Solid State* **8**, 2854–2856 (1967).
14. J. B. Pendry, *Phys. Rev. Lett.* **85**, 3966–3969 (2000).
15. R. A. Shelby, D. R. Smith, S. Schultz, *Science* **292**, 77–79 (2001).
16. V. M. Shalaev, *Nat. Photonics* **1**, 41–48 (2007).
17. N. Fang, H. Lee, C. Sun, X. Zhang, *Science* **308**, 534–537 (2005).
18. A. K. Popov, V. M. Shalaev, *Appl. Phys. B* **84**, 131–137 (2006).
19. A. K. Popov, V. M. Shalaev, *Opt. Lett.* **31**, 2169–2171 (2006).
20. A. K. Popov, S. A. Myslivets, V. M. Shalaev, *Opt. Lett.* **34**, 1165–1167 (2009).
21. M. Scalora *et al.*, *Opt. Express* **14**, 4746–4756 (2006).
22. A. Rose, D. Huang, D. R. Smith, *Phys. Rev. Lett.* **107**, 063902 (2011).
23. S. Tang *et al.*, *Opt. Express* **19**, 18283–18293 (2011).
24. K. M. Dani *et al.*, *Nano Lett.* **9**, 3565–3569 (2009).
25. A. Minovich *et al.*, *Appl. Phys. Lett.* **100**, 121113 (2012).
26. J. Reinhold *et al.*, *Phys. Rev. B* **86**, 115401 (2012).
27. S. M. Barnett, *Phys. Rev. Lett.* **104**, 070401 (2010).
28. N. Dudovich, D. Oron, Y. Silberberg, *Nature* **418**, 512–514 (2002).
29. K. O'Brien *et al.*, *Opt. Lett.* **37**, 4089–4091 (2012).

Acknowledgments: Supported by the U.S. Department of Energy, Office of Basic Energy Sciences, under contract no. DE-AC02-05CH11231 through the Materials Sciences Division of Lawrence Berkeley National Laboratory. H.S. and Z.J.W. acknowledge partial support by the Fulbright Foundation. We thank the Molecular Foundry, Lawrence Berkeley National Laboratory, for technical support in nanofabrication.

Supplementary Materials

www.sciencemag.org/content/342/6163/1223/suppl/DC1
Materials and Methods
Figs. S1 to S8
References (*30–33*)

6 August 2013; accepted 21 October 2013
10.1126/science.1244303

Interfollicular Epidermal Stem Cells Self-Renew via Autocrine Wnt Signaling

Xinhong Lim,[1]* Si Hui Tan,[2] Winston Lian Chye Koh,[3] Rosanna Man Wah Chau,[3] Kelley S. Yan,[4] Calvin J. Kuo,[4] Renée van Amerongen,[1]† Allon Moshe Klein,[5]‡ Roel Nusse[1]‡

The skin is a classical example of a tissue maintained by stem cells. However, the identity of the stem cells that maintain the interfollicular epidermis and the source of the signals that control their activity remain unclear. Using mouse lineage tracing and quantitative clonal analyses, we showed that the Wnt target gene *Axin2* marks interfollicular epidermal stem cells. These *Axin2*-expressing cells constitute the majority of the basal epidermal layer, compete neutrally, and require Wnt/β-catenin signaling to proliferate. The same cells contribute robustly to wound healing, with no requirement for a quiescent stem cell subpopulation. By means of double-labeling RNA in situ hybridization in mice, we showed that the *Axin2*-expressing cells themselves produce Wnt signals as well as long-range secreted Wnt inhibitors, suggesting an autocrine mechanism of stem cell self-renewal.

Stem cells residing in the adult interfollicular epidermis (IFE) regenerate the skin, but the nature of these cells and the molecular signals that regulate them remain incompletely understood. Because of their well-established importance in stem cell maintenance and hair growth, Wnts are candidate self-renewal factors for IFE stem cells. However, Wnt/β-catenin signaling is generally thought to control IFE differentiation rather than self-renewal (*1*, *2*). Reinforcing this view, interfollicular epidermal stem cells (IFESCs) have recently been suggested to originate from more primitive Wnt-independent (Lgr6$^+$) stem cells residing in the hair follicle (*3*). We sought to dissect the role of Wnt signaling in IFE homeostasis and regeneration. Because tissue stem cells are commonly influenced by signals secreted by nearby "niche" cells (*4*), we examined the presence of Wnts and Wnt inhibitors in the skin.

To determine whether Wnt-responding cells are present in the IFE, we looked in mouse skin for cells expressing *Axin2*, a well-known Wnt/β-catenin target gene. We focused on the mouse hindpaw (plantar) epidermis, a region devoid of hair follicles and sweat ducts (fig. S1A). We marked *Axin2*-expressing cells using Axin2-CreERT2 and found labeled cells in the basal layer (Fig. 1A and fig. S1E), consistent with Axin2 mRNA and reporter gene expression (fig. S1, B to D). These labeled cells generated clones in multiple IFE compartments that persisted for up to a year (Fig. 1A and fig. S1F), demonstrating that Axin2-CreERT2–labeled keratinocytes are self-renewing stem cells.

Recent studies examining epidermal stem cell fate provide little indication of the signaling pathways involved in cell fate choice. Using Axin2-CreERT2 as a combined lineage tracing and Wnt reporter tool, we studied the effect of Wnt signaling on cell fate, by analyzing labeled clones at high resolution in whole-mounted epidermis of Axin2-CreERT2/Rosa26-Rainbow (*5*) mice [Fig. 1B and supplementary theory (ST) section S-II]. We first asked whether long-lived Axin2-CreERT2–labeled clones might derive from slow-cycling stem cells that divide with invariant asymmetry to produce transit-amplifying cells (*6*, *7*), or equivalent "committed progenitors" and stem cells that divide with probabilistic fate (*8*–*10*). If Axin2-CreERT2 labeled only slow-cycling stem cells dividing with invariant asymmetry, we would expect to see labeled single cells that divide rarely and eventually give rise to stable, long-lived clones. In contrast, the probabilistic differentiation and self-renewal of stem cells and committed progenitors would lead to a rapid drop in the number of clones as a result of neutral clonal competition, with a concomitant increase in the average size of persisting clones to compensate for those that are lost (*11*). In addition, within a few cell divisions, the size distribution of the persisting clones would follow a simple exponential curve. Comparing the clonal data to these predictions, we found that the labeled Wnt-responding cells and their progeny exhibited all of the characteristics of probabilistic fate and neutral clonal competition (Fig. 1, C and D; fig. S2, A to C; and ST S-III and S-IV).

To determine whether active Wnt signaling, as indicated by *Axin2* expression, occurs in a functionally distinct subpopulation of IFESCs, we examined the number of Axin2-CreERT2–labeled cells in the basal layer over time. Between 3 days and 5 months after initial labeling, the total number of labeled cells in the basal layer of the epidermis remained constant (Pearson correlation coefficient $R = 0.08$ to time after labeling) (Fig. 1E and fig. S2H). This indicates that both Axin2-CreERT2–labeled and unlabeled cells have equal self-renewal capacity in homeostasis, suggesting that all IFESCs express *Axin2* (fig. S1, B to D), but only a subset is labeled when treated with

[1]Department of Developmental Biology, Howard Hughes Medical Institute (HHMI), Institute for Stem Cell Biology and Regenerative Medicine, School of Medicine, Stanford University, Stanford, CA, USA. [2]Program in Cancer Biology, School of Medicine, Stanford University, Stanford, CA, USA. [3]Department of Bio-engineering, Stanford University, Stanford, CA, USA. [4]Department of Medicine, School of Medicine, Stanford University, Stanford, CA, USA. [5]Department of Systems Biology, Harvard Medical School, Boston, MA, USA.

*Present address: Institute of Medical Biology, A*STAR, Singapore.
†Present address: Swammerdam Institute for Life Sciences, University of Amsterdam, Netherlands.
‡Corresponding author. E-mail: rnusse@stanford.edu (R.N.); allon_klein@hms.harvard.edu (A.M.K.)

Tamoxifen. Further supporting the notion that *Axin2*-expressing cells are representative of the general population of IFESCs, clonal outcomes showed the same probabilities of division and differentiation at early and late time points (fig. S2, D and E, and ST S-V). Thus, Axin2-CreERT2–labeled cells were not biased in their fate choice and were not enriched in a subpopulation of slow-cycling stem cells. If slow-cycling IFESCs are present, they too undergo neutral competition (ST S-VI). However, using a DNA label–retaining assay (*12*, *13*) (fig. S3A), we were unable to detect any label-retaining cells in or outside of persisting Axin2-CreERT2–labeled clones (Fig. 1, F and G; fig. S3, B to E; and ST S-VI).

To further test the regenerative potential of *Axin2*-expressing IFESCs, we induced full-thickness skin biopsy punch wounds in labeled Axin2-CreERT2/Rosa26-mTmG^{flox} mice (fig. S4A). We found large numbers of relatively even-sized clones radiating into the healed epidermis that persisted for up to 35 days (Fig. 2A and fig. S4B), showing that *Axin2*-expressing IFESCs robustly contribute to regeneration. However, the labeled cells constituted similar percentages of injured and uninjured skin (Fig. 2B and fig. S4C), indicating that labeled and unlabeled cells have equal abilities to regenerate. Consistent with data from our cell label–retention assays (Fig. 1, F and G; fig. S3; and ST S-VI), these results also indicate

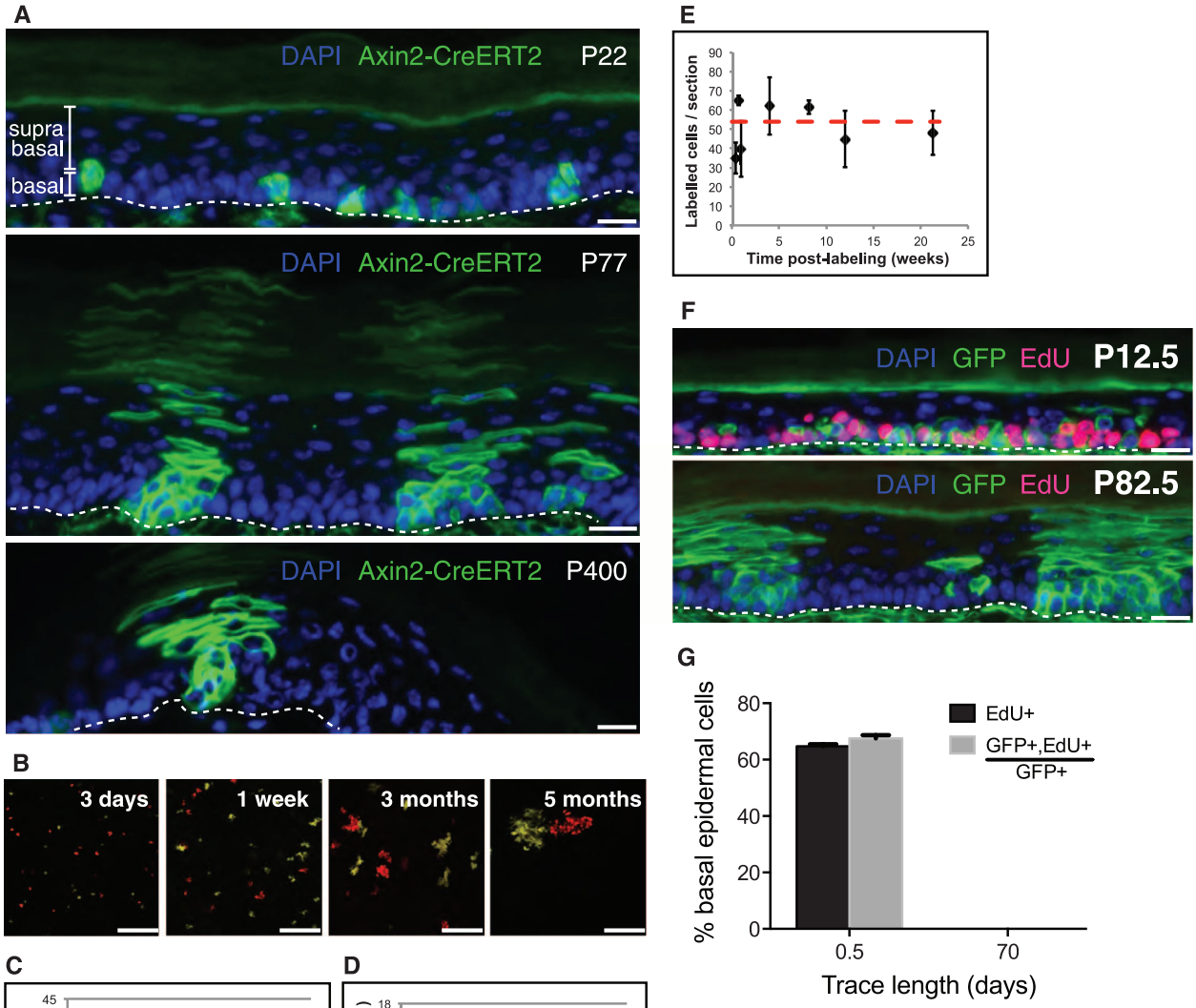

Fig. 1. *Axin2*-expressing basal interfollicular epidermal cells are stem cells that undergo neutral competition and exhibit probabilistic cell fate. (**A**) Histological sections of plantar epidermis from Axin2-CreERT2/Rosa26mTmG^{flox} mice chased for 1 day [postnatal day 22 (P22)], 2 months (P77), and more than 1 year (P400). Scale bars, 10 μm. Basal and suprabasal epidermal layers are indicated. The dashed line denotes the approximate location of the epidermis/dermis boundary. (**B**) Representative images of whole-mounted Axin2-CreERT2/Rosa26-Rainbow^{flox} plantar epidermis traced from 3 days to 5 months. Only mOrange and mCherry clones in the basal epidermal layer are shown and scored (ST S-II). Scale bars, 100 μm. (**C** and **D**) The number of clones per image section drops, whereas the average clone size (basal cells per clone) increases, consistent with a model of probabilistic stem cell fate and neutral competition (NC model, red curve) (error bars = SD, $n \geq 3$ mice). (**E**) The number of labeled basal cells per image section remains stable; the red dashed line shows the average over all time points. (**F**) Representative histological sections of Axin2-CreERT2/Rosa26mTmG^{flox} plantar epidermis chased for 0.5 days (P12.5) and 70.5 days (P82.5). The dashed line denotes the approximate location of the epidermis/dermis boundary. Scale bars, 10 μm. (**G**) Changes in the proportion of EdU$^+$ and GFP$^+$, EdU$^+$/GFP$^+$ basal cells (error bars indicate SEM). All counts were derived from $n \geq 2$ animals per time point and were subject to unpaired Student's *t* tests.

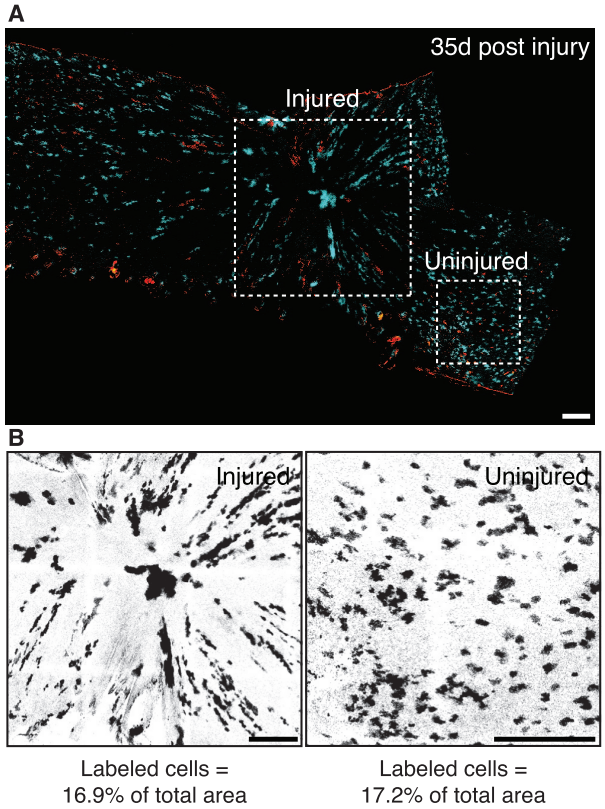

Fig. 2. *Axin2*-expressing interfollicular epidermal stem cells contribute robustly to wound repair. (A) Whole-mount views of healing Axin2-CreERT2/Rosa26-Rainbow^{flox} plantar epidermis at 35 days after wounding. Dashed squares denote approximate injured (left) and uninjured (right) areas. **(B)** Image masks of injured and uninjured areas. Scale bars, 300 μm.

that, if they are present, rare slow-cycling stem cells are not the primary contributors to epidermal wound repair as previously suggested (*10*).

We next tested whether *Axin2*-expressing IFESCs functionally require Wnt/β-catenin signaling, by conditionally inactivating the gene encoding β-catenin in *Axin2*-expressing cells. We found an average 30% reduction in the overall cellularity of mutant epidermises (Fig. 3, A and B). Consistent with this, 68 ± 3% of control basal cells expressed Ki67 (Fig. 3, C and D), a marker of proliferating cells, whereas only 35 ± 4% of mutant basal cells were Ki67-positive (Fig. 3, C and D), suggesting a proliferation defect. Similarly, the number of basal cells expressing phosphohistone-H3, another marker of dividing cells, was significantly decreased (fig. S5, A and B). To determine whether epidermal differentiation was also affected, we stained skins for Keratin-10 (K10), an early marker of keratinocyte differentiation. Only 18 ± 1% of control basal cells expressed K10, consistent with estimates obtained from clonal analysis (ST S-IV), whereas 36 ± 1% of mutant basal cells were K10-positive (Fig. 3, E and F). Although we cannot exclude systemic effects, our results suggest that IFESCs that are mutant for β-catenin stop proliferating and undergo differentiation. Taken together with our clonal analysis, this suggests that Wnt/β-catenin signal-

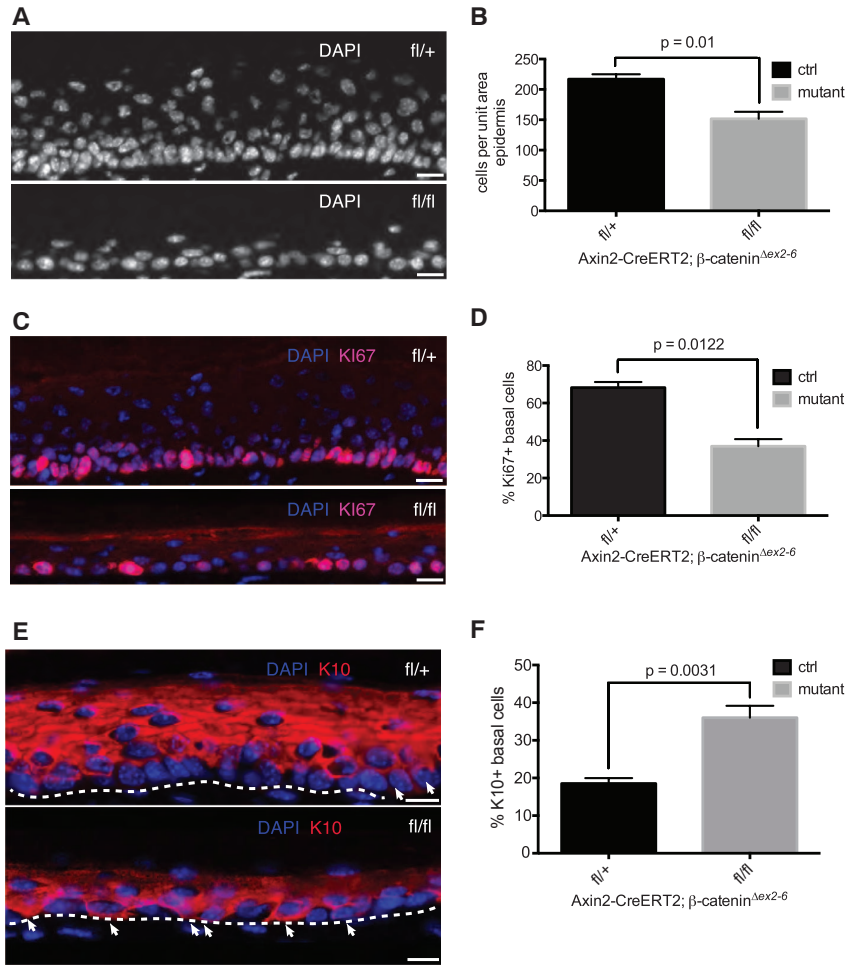

Fig. 3. *Axin2*-expressing interfollicular epidermal stem cells require β-catenin to proliferate and maintain normal epidermal homeostasis. (A, **C**, and **E)** Representative images of DAPI, Ki67, and K10 immunostaining of control Axin2-CreERT2/β-catenin$^{\Delta ex2-6-fl/+ \text{ or } -del/+}$ and mutant Axin2-CreERT2/β-catenin$^{\Delta ex2-6-fl/fl \text{ or } -fl/del}$ plantar epidermis. White arrows in (E) indicate basal epidermal cells staining positive for K10. Dashed lines denote the approximate location of the epidermis/dermis boundary. **(B**, **D**, and **F)** Changes in cellularity, proliferative index, and differentiation between control and mutant plantar epidermises as determined by counting and plotting (B) DAPI$^+$ nuclei, (D) Ki67$^+$ nuclei, and (F) K10$^+$ basal cells (error bars indicate SEM). All counts were derived from $n \geq 3$ independent experiments and were subject to pairwise Student's *t* tests. Scale bars, 10 μm.

ing maintains the IFE stem cell proliferative state but does not affect the likelihood of symmetric self-renewal or differentiation of individual cells.

So where do the Wnt signals come from, and how is the niche for IFESCs organized in a way that permits neutral competition? With the use of double-labeling RNA in situ hybridization, we found that *Axin2*-expressing basal cells in the postnatal epidermis are themselves the source of Wnt signals, expressing several Wnt genes, including *Wnt4* and *Wnt10a* (Fig. 4A and fig. S6B). This pattern of Wnt gene expression is consistent with previous reports regarding the embryonic basal epidermis (*14*, *15*). Further supporting this observation, primary basal epidermal cells isolated from human skin express *Wnt4*, whereas suprabasal epidermal cells do not (Fig. 4B) (*16*). Similarly, cultured primary adult human epidermal keratinocytes express various Wnt genes, as well as *Porcupine* (*Porcn*), which is required for Wnt secretion (fig. S7).

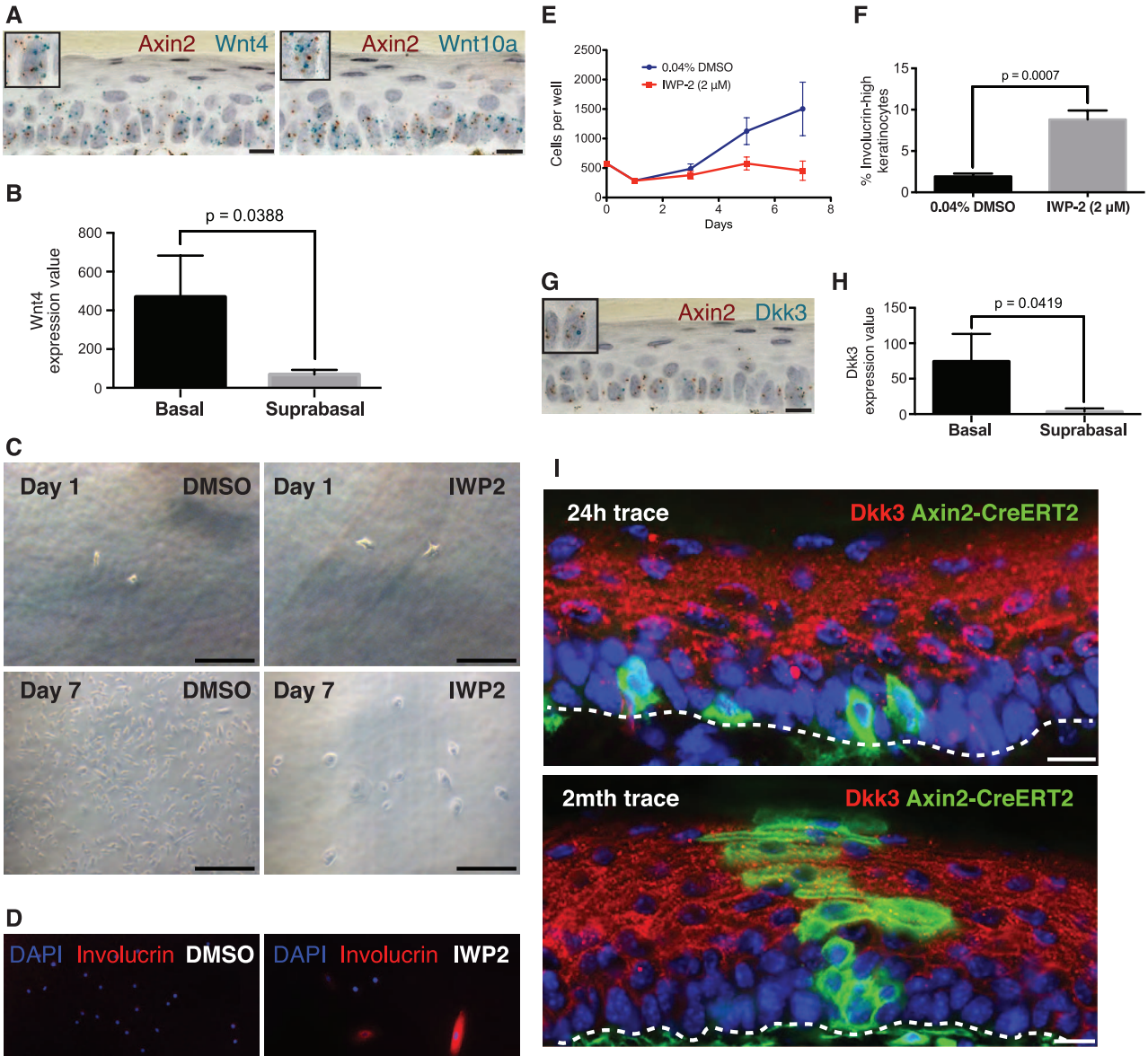

Fig. 4. *Axin2*-expressing interfollicular epidermal stem cells express Wnt and Dkks. (**A**) Representative images of double-labeling RNA in situ hybridization in mouse plantar epidermis for Axin2 (red spots) and Wnt4 or Wnt10a (turquoise spots). Inset boxes show a magnified view of individual basal cells expressing both Axin2 and Wnts. Scale bars, 10 μm. (**B**) Wnt4 expression in β4-integrin^{+} primary human basal epidermal keratinocytes versus β4-integrin-suprabasal epidermal keratinocytes (error bars indicate SD). Expression values are from the Gene Expression Omnibus (GEO) data set GSE26059. (**C** and **D**) Representative (C) bright-field or (D) immunofluorescence images of keratinocytes continuously cultured in defined medium with either 0.04% DMSO or 2 μM IWP-2, at the beginning (day 1) and the end (day 7) of the experiment, then stained for involucrin. Scale bars, 50 μm (bright-field image) or 100 μm (immunofluorescence image). (**E** and **F**) Changes in the (E) number of cells and (F) percentage of involucrin-high cells per well of keratinocytes treated with either 0.04% DMSO or 2 μM IWP-2 (error bars indicate SEM). Cell counts at all time points were derived from n = 3 replicate wells. (**G**) Representative image of double-labeling RNA in situ hybridization for Axin2 (red spots) and Dkk3 (turquoise spots). The inset box shows a magnified view of individual basal cells expressing both Axin2 and Dkk3. Scale bar, 10 μm. (**H**) Dkk3 expression in primary human β4-integrin$_{+}$ basal epidermal keratinocytes versus β4-integrin-suprabasal epidermal keratinocytes (error bars indicate SD). Expression values are from GEO data set GSE26059. (**I**) Representative images of Dkk3 immunostaining in plantar epidermises of Axin2-CreERT2/Rosa26mTmG^{flox} mice exposed to Tam at P21 and chased for 1 day (P22) and 2 months (P77). Scale bars, 10 μm.

To determine whether IFESCs functionally require the Wnt that they produce, we treated human epidermal keratinocytes with IWP-2, a validated small-molecule inhibitor of Wnt secretion, and cultured them at clonal density in a defined medium. IWP-2–treated keratinocytes were sparsely distributed and became large and flattened with arrested growth, unlike the densely packed, cuboidally shaped, control keratinocytes (Fig. 4, C and E). Many more IWP-2–treated keratinocytes also expressed high levels of involucrin, a marker of advanced keratinocyte differentiation (Fig. 4, D and F). These data are consistent with our in vivo observations that IFESCs undergo premature differentiation upon loss-of-function mutations in Wnt signaling (Fig. 3, E and F).

If IFESCs are both the source and the target of Wnt signals, how might they escape from this autocrine loop and enter a differentiation process? Several genes for secreted Wnt inhibitors, including *Dickkopf-1* (*Dkk1*), *Dkk3*, and *Wnt Inhibitory Factor-1* (*WIF1*) are expressed in the skin (*17–19*). With double-labeling RNA in situ hybridization, we saw overlapping expression of *Dkks* and *Axin2* expression in basal cells (Fig. 4G and fig. S6C). This is similar to the situation in human skin, in which primary human basal cells, either isolated from skin tissue or cultured in vitro, express *Dkks* (Fig. 4H and fig. S7). Although the Dkk (Fig. 4, G and H, and fig. S6C) and WIF1 (*19*) mRNAs are mostly located in basal cells, the secreted WIF1 and Dkk3 proteins accumulate at high levels in the suprabasal layers (*18*, *19*). By antibody staining for the Dkk3 protein, we confirmed that Dkk3 is localized to the suprabasal layers, directly adjacent to the *Axin2*-expressing basal progenitors (Fig. 4I and figs. S8, A and B, and S9) (*18*). We tested whether Dkk influences stem cells in the skin by adenoviral overexpression of Dkk, finding that this caused a thinned and hypoproliferative epidermis (fig. S10) resembling β-catenin mutant skin (Fig. 3A). These data suggest that the differential diffusion of Wnts and Dkk from the basal epidermal stem cells may restrict autocrine Wnt/β-catenin signaling to the basal layer of the epidermis (fig. S8C). IFESCs leaving the basal layer would encounter increased Wnt inhibitors and differentiate.

Functional redundancy between the various Wnt inhibitors and Wnts expressed in the skin (Fig. 4, A and G, and fig. S6, B and C) may explain the absence of overt phenotypes in mice mutant for these genes (*20*). However, there is genetic evidence supporting an essential role for Wnt signals in the epidermis. *Porcn*-knockout mice display a thinned epidermis, similar to that seen in human patients bearing *Porcn* mutations who develop focal dermal hypoplasia (*21–23*). Mutations in both Wnt effectors *Tcf3* and *Tcf4* result in a thinner epidermis (*24*), whereas deleting β-catenin using the basal epidermal specific driver Keratin-5-rtTA/tet-O-Cre also results in a thinner and hypoproliferative plantar epidermis (*25*).

Signals emerging from a distinct niche cell compartment are thought to be the main drivers of stem cell self-renewal. We find that epidermal stem cells themselves can be the source of their own self-renewing signals and differentiating signals for their progeny. We postulate that the multiplicity of Wnts and Wnt inhibitors produced by epidermal stem cells allows for fine-tuning of epidermal thickness and wound repair.

References and Notes

1. J. Huelsken, R. Vogel, B. Erdmann, G. Cotsarelis, W. Birchmeier, *Cell* **105**, 533–545 (2001).
2. S. Beronja *et al.*, *Nature* **501**, 185–190 (2013).
3. H. J. Snippert *et al.*, *Science* **327**, 1385–1389 (2010).
4. V. P. Losick, L. X. Morris, D. T. Fox, A. Spradling, *Dev. Cell* **21**, 159–171 (2011).
5. H. Ueno, I. L. Weissman, *Dev. Cell* **11**, 519–533 (2006).
6. I. C. Mackenzie, *Nature* **226**, 653–655 (1970).
7. C. S. Potten, *Cell Tissue Kinet.* **7**, 77–88 (1974).
8. E. Clayton *et al.*, *Nature* **446**, 185–189 (2007).
9. D. P. Doupé, A. M. Klein, B. D. Simons, P. H. Jones, *Dev. Cell* **18**, 317–323 (2010).
10. G. Mascre *et al.*, *Nature* **489**, 257–262 (2012).
11. A. M. Klein, B. D. Simons, *Development* **138**, 3103–3111 (2011).
12. J. R. Bickenbach, J. McCutecheon, I. C. Mackenzie, *Cell Prolif.* **19**, 325–333 (1986).
13. K. M. Braun *et al.*, *Development* **130**, 5241–5255 (2003).
14. S. Reddy *et al.*, *Mech. Dev.* **107**, 69–82 (2001).
15. F. Witte, J. Dokas, F. Neuendorf, S. Mundlos, S. Stricker, *Gene Expr. Patterns* **9**, 215–223 (2009).
16. N. Radoja, A. Gazel, T. Banno, S. Yano, M. Blumenberg, *Physiol. Genomics* **27**, 65–78 (2006).
17. Y. Yamaguchi *et al.*, *J. Cell Biol.* **165**, 275–285 (2004).
18. G. Du *et al.*, *Exp. Dermatol.* **20**, 273–277 (2011).
19. H. Schlüter, H.-J. Stark, D. Sinha, P. Boukamp, P. Kaur, *J. Invest. Dermatol.* **133**, 1669–1673 (2013).
20. I. del Barco Barrantes *et al.*, *Mol. Cell. Biol.* **26**, 2317–2326 (2006).
21. J. J. Barrott, G. M. Cash, A. P. Smith, J. R. Barrow, L. C. Murtaugh, *Proc. Natl. Acad. Sci. U.S.A.* **108**, 12752–12757 (2011).
22. W. Liu *et al.*, *PLOS ONE* **7**, e32331 (2012).
23. J. L. Bolognia, J. L. Jorizzo, J. V. Schaffer, in *Dermatology* (Mosby-Saunders, London, 2012), pp. 869–885.
24. H. Nguyen *et al.*, *Nat. Genet.* **41**, 1068–1075 (2009).
25. Y. S. Choi *et al.*, *Cell Stem Cell* 10.1016/j.stem.2013.10.00 (2013).

Acknowledgments: These studies were supported by the HHMI, California Institute of Regenerative Medicine grant TR1-01249, and NIH grants NIH 1U01DK085527, 1R01DK085720, and 5K08DK096048. We thank L. De Simone, A. E. Marcy, and P. H. Chia for cell quantification assistance; C. Logan, S. J. Habib, and A. Oro for manuscript comments; and J. Akech and L.-C. Wang at Advanced Cell Diagnostics for assistance with RNA in situ hybridization. X.L., S.H.T., W.L.C.K., and R.M.W.C. are supported by National Science Scholarships from A*STAR, Singapore. A.M.K. holds a Career Award at the Scientific Interface from the Burroughs Wellcome Fund. K.S.Y. has a Burroughs Wellcome Fund Career Award for Medical Scientists. R.v.A. was supported by a European Molecular Biology Organization long-term fellowship (ALTF 122-2007) and a Dutch Cancer Society fellowship.

Supplementary Materials

www.sciencemag.org/content/342/6163/1226/suppl/DC1
Materials and Methods
Supplementary Theory and Data Analysis
Figs. S1 to S10
References (*26–40*)

29 April 2013; accepted 28 October 2013
10.1126/science.1239730

Preferential Recognition of Avian-Like Receptors in Human Influenza A H7N9 Viruses

Rui Xu,[1] Robert P. de Vries,[2] Xueyong Zhu,[1] Corwin M. Nycholat,[2] Ryan McBride,[2] Wenli Yu,[1] James C. Paulson,[2]* Ian A. Wilson[1,3]*

The 2013 outbreak of avian-origin H7N9 influenza in eastern China has raised concerns about its ability to transmit in the human population. The hemagglutinin glycoprotein of most human H7N9 viruses carries Leu^{226}, a residue linked to adaptation of H2N2 and H3N2 pandemic viruses to human receptors. However, glycan array analysis of the H7 hemagglutinin reveals negligible binding to humanlike α2-6–linked receptors and strong preference for a subset of avian-like α2-3–linked glycans recognized by all avian H7 viruses. Crystal structures of H7N9 hemagglutinin and six hemagglutinin-glycan complexes have elucidated the structural basis for preferential recognition of avian-like receptors. These findings suggest that the current human H7N9 viruses are poorly adapted for efficient human-to-human transmission.

In the spring of 2013, an outbreak of human infections caused by avian-origin H7N9 subtype influenza A virus occurred in the eastern provinces of China (*1*). By the end of May 2013, 132 cases of laboratory-confirmed H7N9 influenza were reported, resulting in 37 deaths (*2*). These patients generally presented influenza-like illnesses that frequently progressed to acute respiratory distress syndrome and severe pneumonia (*3*, *4*). However, natural infection by H7N9 viruses in avian hosts are asymptomatic, which allows the virus to spread among birds and not be readily detected by surveillance (*2*).

The H7N9 outbreak has raised concerns about its potential for causing human pandemics or epidemics (*5*, *6*). Compared with H5N1 viruses, H7N9 appears to transmit from birds to humans more readily, with reports of a relatively large